Available online at www.sciencedirect.com
ScienceDirect
Biochemical and Biophysical Research Communications 364 (2007) 195–200
BBRC
www.elsevier.com/locate/ybbrc

The mistletoe lectin I—Phloretamide structure reveals a new function of plant lectins

A. Meyer [a], W. Rypniewski [b], L. Celewicz [c], V.A. Erdmann [d], W. Voelter [e], T.P. Singh [f], N. Genov [g], J. Barciszewski [b], Ch. Betzel [a,*]

[a] *Institute of Biochemistry and Molecular Biology, University of Hamburg, c/o DESY, Notkestr. 85, Building 22a, 22603 Hamburg, Germany*
[b] *Institute of Bioorganic Chemistry of the Polish Academy of Sciences, Noskowskiego 12, 61-704 Poznan, Poland*
[c] *Faculty of Chemistry, Adam Mickiewicz University, Grunwaldzka 6, 60-780 Poznan, Poland*
[d] *Institute of Chemistry and Biochemistry, Free University Berlin, Thieallee 63, 14195 Berlin, Germany*
[e] *Institute of Physiological Chemistry, University of Tübingen, Hoppe-Seyler-Strasse 4, 72076 Tübingen, Germany*
[f] *Department of Biophysics, All India Institute of Medical Sciences, New Delhi, India*
[g] *Institute of Organic Chemistry, Bulgarian Academy of Sciences, Sofia, Bulgaria*

Received 15 September 2007
Available online 5 October 2007

Abstract

The X-ray structure at 2.7 Å resolution of the complex between the European mistletoe lectin I (*Viscum album*, ML-I) and the plant growth hormone, 3-(*p*-hydroxyphenyl)-propionic acid amide (phloretamide, PA) from xylem sap has revealed the binding of PA at the so far undescribed hydrophobic cavity located between the two subunits of this ribosome-inhibiting protein. No such cavity is observed in related lectins. The binding of PA is achieved through interactions with the non-conserved residues Val228A, Leu230A, Arg388B, and the C-terminal Pro510B. It is conceivable that binding of PA to ML-I is part of a defence mechanism of the parasite against the host, whereby the parasite prevents the growth hormone of the host from interfering with its own regulatory system. The specific binding of PA to ML-I indicates that heterodimeric RIPs are multifunctional proteins whose functions in the cell have not yet been fully recognized and analyzed.

Keywords: *Viscum album*; Plant growth hormone; X-ray analysis

The European mistletoe (*Viscum album*) is a semi-parasitic plant widely spread over Europe and parts of Asia. It contains at least three lectins: I, II, and III (ML-I–III) [1]. ML-I consists of two subunits (A and B) and belongs to the family of ribosome inactivating proteins, type II (RIP-type II). Subunit A catalyses the hydrolysis of the *N*-glycosidic bond of adenosine 4324 of eukaryotic 28S rRNA [2] while subunit B, owing to its galactose recognizing ability, is required for endocytosis of subunit A, after which its toxicity is deployed. It has been suggested that ML-I is part of a defence system against insects, bacteria, and fungi [3]. An aqueous extract of *V. album* is already used in therapeutics and ML-I has been identified as its main active component [4].

The European mistletoe resides on the aerial axis of higher plants, where it penetrates the host tissue by specialized roots, thus tapping the transpiration stream across the xylem–xylem connections. The transpiration per leaf surface is 1.5- to 7.5-fold higher than that of the host [5,6] with deleterious consequences for the growth of the host. Such high transpiration rate is a common feature of hemiparasites and is evident for the import of xylem water from the host system. The flow is achieved via a combination of transpiration and accumulated solved substances within the mistletoe tissue, e.g. potassium and sodium [7]. In consequence, mistletoe assimilates and also accumulates some organic substances transported by xylem tissue [8].

* Corresponding author. Fax: +49 40 8998 4747.
E-mail address: Betzel@unisgi1.desy.de (Ch. Betzel).

0006-291X/$ - see front matter © 2007 Elsevier Inc. All rights reserved.
doi:10.1016/j.bbrc.2007.09.113

3-(*p*-Hydroxyphenyl)-propionic acid amide (phloretamide, PA) has been identified in xylem sap of *Malus domestica* with mass spectroscopy and NMR spectroscopy. It moves upward in young apple trees at blossom time. PA is found during the period of six weeks from the middle of May until the end of June, which indicates a role in seasonal plant development [9].

Here we report the X-ray structure of the ML-I in a complex with PA that reveals its ordered binding at a pocket between subunits A and B. These results, together with our earlier analysis of ML-I complexes with adenine and galactose [10,11], raise the question of the role of lectins within the cellular signalling system. It appears that ML-I is a multifunctional protein with a regulatory potential.

Materials and methods

Protein purification. Mistletoe lectin I was purified for crystallization following previously described procedures [1]. Small branches and leaves of the European mistletoe (*V. album*) growing on apple trees (*M. domestica*) were used. The crude material was collected in the period February–March. Flash-frozen tissues were ground into powder, dissolved in water, and centrifuged. The supernatant was loaded on an affinity column of lactose immobilized with divinyl sulfone [12]. Lectins were separated using aminophenyl-boronic-acid-affinity chromatography [13]. For crystallization ML-I was dialyzed against 0.2 M glycine–HCl buffer at pH 2.5, as described before [10].

Crystallization. For crystallization experiments the following solutions were prepared: buffer C (0.2 M glycine–HCl, pH 2.5 saturated with PA), buffer G (10 mM Tris–HCl, pH 2.5, 0.1% LMP-agarose, and 0.5 M NaCl). The protein was dissolved in 0.2 M glycine–HCl, pH 2.5 to a concentration of 4 mg/ml. The LMP-agarose was heated to 90 °C for 10 min. Crystallization experiments were carried out using the sitting drop vapour diffusion method. The reservoir solution contained 250 µl of glycine–HCl, pH 2.5, 175 µl of solution S (3.9 M ammonium sulfate in 125 µl of H_2O) and buffer G. 2 µl of buffer G were used to prevent sedimentation of crystals in order to improve the diffraction quality. The crystallization drop contained 2.6 µl protein solution, 1.2 µl buffer C, 6 µl buffer G, and 0.6 µl buffer S. Hexagonal–bipyramidal crystals of ML-I grew up to the final size of 0.2–0.3 mm in approx. two weeks at 20 °C.

Data collection and processing. X-ray diffraction data were collected up to 2.7 Å resolution using a 165 mm MAR CCD detector at the consortium beam line X13 (HASYLAB/DESY), using crystals frozen and stabilized at 100 K. Prior to flash freezing crystals were soaked in a cryoprotectant solution containing 25% v/v glycerol in the reservoir solution saturated with PA. Data processing and data scaling were carried out using DENZO and SCALEPACK [14]. The crystals belong to the space group $P6_522$ with a single ML-I molecule in the asymmetric unit. Unit cell parameters were $a = 107.2$ Å and $c = 312.4$ Å. The packing parameter V_M was calculated to be 4.4 Å/Da [15], which corresponded to a solvent content of 75%. Data collection and scaling statistics are summarized in Table 1.

Structure determination and refinement. The structure of the ML-I–AMP complex (PDB ID: 1M2T) was used after removing the solvent and ligand atoms for the initial model building and refinement. Further refinement, using all data up to 2.7 Å resolution, was carried out applying the program REFMAC 5 [16,17]. A subset of 5% of the reflections was used only for the R_{free} statistics [18]. Manual rebuilding of the model and electron intensity interpretation was done using the graphics program COOT [19]. Ligand molecules were identified using maps calculated with the coefficients $F_o - F_c$. The electron density was also visualized using $2F_o - F_c$ maps. ML-I is known to have four potential NAG *N*-glycosylation sites, characterized by sequence motifs Asn-X-Ser/Thr [1]. The sites are at Asn112 in subunit A and Asn308, Asn343, and Asn383 in subunit B. In the course of the refinement, $F_o - F_c$ maps showed carbohydrate densities at all the four glycosylation sites. However, only one NAG residue could be identified at Asn112 and at Asn308, while two NAG residues were visible at the other two sites. These saccharides were included in the model and subsequently refined. Water molecules were included if observed as spherical peaks at a level of at least 2.5σ in the $F_o - F_c$ difference maps, provided that suitable hydrogen bonding partners were already present in the model. Water molecules that failed to reappear at 1.5σ in $2F_o - F_c$ maps following the subsequent refinement were removed from the model. A bulk solvent model was included in the final stages and resulted in improvement of the *R*-factor, particularly for data in the lowest resolution shell. The structure of the complex was refined to an *R* value of 21.7% and R_{free} of 26.6% for all data between 20.0 and 2.7 Å resolution. The refinement statistics are summarized in Table 1 and the coordinates were deposited at the PDB (PDB ID: 2R9K).

Model analysis. The quality of the final model was assessed using the program PROCHECK [20]. The program SYBYL [21] was used to analyze the internal cavities in the protein model and to calculate their volume. Sequence alignment was done with the program ClustalW [22]. The figures were prepared applying the programs Pymol (http://www.pymol.org), ChemSketch [23], CorelDraw, and CorelPaint (CorelDraw12, Graphics Suite) [24].

Table 1
Details of data collection and refinement parameters

	ML-I–PA complex
X-ray source	DESY, Hamburg, beam line X13
Temperature (K)	100
Resolution range	20–2.7 (2.75–2.70)[a]
Wavelength (Å)	0.8048
Space group	$P6_522$
Cell parameters: $a = b$, c (Å)	107.1, 312.4
No. observations	780,357
No. unique reflections	30,327
R_{merge} (%)[b]	6.0 (47.3)
Completeness (%)	100.0 (100.0)
$I/\sigma(I)$ in high-resolution bin	3.6
Data redundancy	6.3
Final R-factor/R_{free} (%)	21.7/26.6
No. protein atoms	3936
No. solvent molecules	93
No. carbohydrate atoms	88
Other atoms	39
Average B-factors (Å^2)	
Protein	44.7
Solvent	41.1
Overall	44.8
R.m.s.d. from ideal bond length (Å)	0.016
R.m.s.d from ideal bond angles (°)	1.5
Ramachandran plot, % residues in regions:	
Most favored	89.4%
Additionally allowed	10.4%
Generously allowed	0.2%
PDB ID	2R9K

[a] The figures in brackets are for the last resolution shell.

[b] $R_{merge} = \sum_{hkl}\sum_i |I_i(hkl) - \langle I(hkl)\rangle| / \sum_{hkl}\sum_i I_i(hkl)$, where $I_i(hkl)$ and $\langle I(hkl)\rangle$ are the observed individual and mean intensities of a reflection with the indices hkl, respectively, $\sum_i$ is the sum over i measurements of a reflection with the indices hkl, and $\sum_{hkl}$ is the sum over all reflections.

Results and discussion

Overall crystal structure and model quality

The final X-ray structure consisted of a single ML-I molecule, one molecule of PA, and 93 ordered water molecules. The protein model consisted of 510 amino acid residues in two chains (chain A, 1–248 and chain B, 249–510) and 6 glycan residues at four glycosylation sites. The overall structure is shown in Fig. 1. Chain A is folded into three domains. Domain I (amino acid residues 1–109) is rich in β-structures while domain II (residues 110–198) consists mainly of α-helices. Domain III of chain A interacts with chain B through its β-sheet structure with one α-structure (residues 199–249). The B chain consists of two globular domains, presumably a result of gene duplication, similar to those reported for ricin [25]. Each domain has a galactose-specific binding site but not all residues involved in sugar binding are identical in both binding sites. ML-I is an example for a lectin in which sugar-binding sites differ within one single chain [11]. The program PROCHECK was used to validate the quality of the final structure [20]. 89% of the residues were found in the most favored regions of the Ramachandran plot and the remaining residues were in the additionally allowed regions. Details of the data statistics and refinement are summarised in Table 1.

PA binding

Clear electron density, corresponding to a single molecule of PA was observed in a cavity located at the interface between chains A and B (Fig. 1). The ligand could be interpreted unambiguously, using the $F_o - F_c$ map contoured at 3σ level (Fig. 2A and B). The PA-binding cavity is defined by residues from domain III of chain A and residues from both domains of chain B. PA was refined at full occupancy with temperature factors comparable to those of the surrounding protein atoms. The phenyl ring of PA is located between the side chains of Val228A, Leu230A, Arg388B, and the C-terminal Pro510B. The propionic group is located between Asp235A and Thr390B and the carbonyl oxygen atom interacts with a water molecule located inside the cavity (O–O distance 2.6 Å). The amide group of PA interacts with the carbonyl oxygen of Arg234A (N–O distance 3.4 Å). A glycerol molecule, from the cryoprotectant solution, is visible nearby with its 2′ hydroxyl oxygen located 3.5 Å from the PA amide group. A comparison with the structure of ML-I in a complex with adenine monophosphate (PDB ID: 1M2T), which has an empty PA-binding cavity, revealed that PA binding does not induce a significant conformational change in the protein structure.

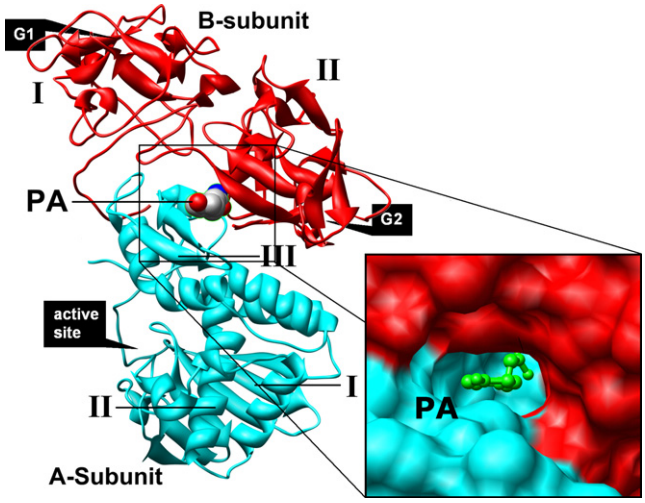

Fig. 1. Ribbon representation of the structure of ML-I–PA complex. The two globular domains of subunit B, labelled I and II, are located above and colored in red. The galactose binding sites are labelled G1 and G2. The A-chain below, colored in cyan, consists of three domains: I, II, and III. The active site, which catalyses the depurination of A4324 of 28S rRNA, is formed by residues of the A-subunit. The PA molecule is shown in surface presentation and the zoomed PA-binding cavity, which is almost in the central part of the interface between A and B chain, is shown as well. (For interpretation of the references to colors in this figure legend, the reader is referred to the web version of this article.)

The active site

A comparison of the native active site and the respective region in the structure of ML-I complexed with adenine at the active site, revealed significant differences in the protein conformation around this site. In the complex Tyr76 and Tyr115 form distinct ring-stacking interactions with the adenine moiety, whereas in the ML-I–PA complex the side chain of Tyr115 is rotated by approx. 120° and turned away from the vacant adenine-binding cavity and interacts via its hydroxyl group with a sulfate ion. The ion, in addition to the H-bond with Tyr115, is further coordinated through interactions with His124, Arg125, and Asp126. The imidazole ring of His124 is rotated approx. 90° relatively to the ML-I–adenine complex, in order to form an H-bond with the sulfate.

Internal cavities

The structure analysis revealed that the PA-binding site forms a deep cavity extending between the two globular domains of chain B. The cavity is formed by approx. 30 residues and its calculated volume is approx. 170 $Å^3$. No comparable internal cavities were found in other parts of the molecule, e.g. the active site in chain A with a volume of approx. 30 $Å^3$. In ricin (PDB ID: 2AAI), a similar cavity was also found between the two domains of the B chain and the volume was calculated to be approx. 185 $Å^3$, but the entrance to the cavity was quite different from that found in ML-I (see below). In abrin A (PDB ID: 1ABR) a small internal cavity of about 90 $Å^3$ and for ebulin I (PDB ID: 1HWM) a cavity of about 20 $Å^3$ were identified in the same region of the structure.

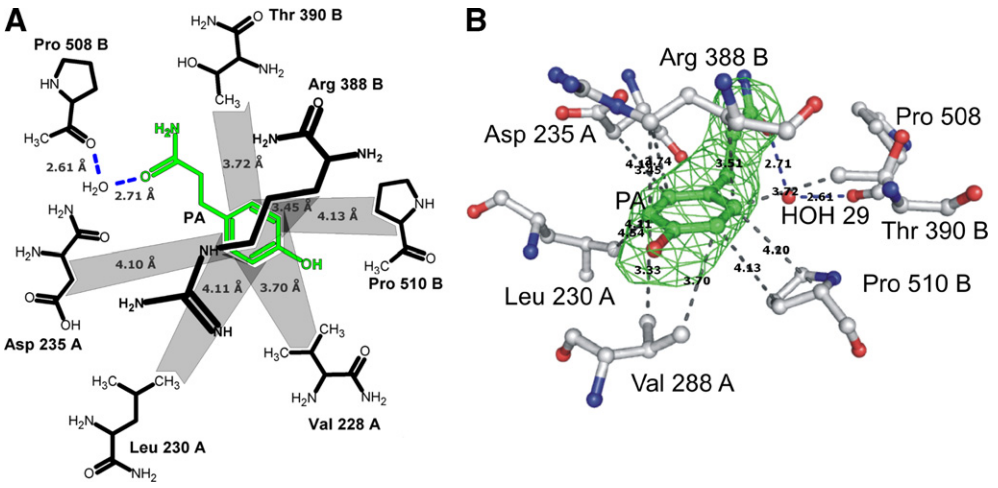

Fig. 2. (A) Scheme showing the interactions between PA (light green) and protein residues in the PA-binding site of ML-I. Protein residues within a radius of 4.5 Å of PA are included. Pro510B is the C-terminus of the B chain and its location is close to the interface zone between the ML-I A- and B-subunit. Hydrophobic interactions between ML-I and PA are shown as grey filled out areas and hydrogen bonds are shown as blue dashed lines. Hydrogen bonds with the carbonyl group of Pro508B take place via a solvent water molecule 29. (B) View of the PA (green) binding site of ML-I. The binding pocket is formed by residues of both chains. Dark blue dashed lines indicate intermolecular hydrogen bonds between PA and the protein or water. Dark grey dashed lines indicate van der Waals interactions between PA and amino acid residues. The $F_o - F_c$ omit map for PA is shown with a cut-off at 3.5σ. (For interpretation of the references to colors in this figure legend, the reader is referred to the web version of this article.)

Sequence and structure comparison

The amino acid sequence of ML-I has been aligned with sequences of lectins from three non-parasitic organisms, whose X-ray structures had been determined [26–28]. The level of sequence identity between ML-I and the other proteins is 48%, 45%, and 38% for ricin, abrin A, and ebulin I, respectively.

For the A-subunit, 22% and for the B-subunit 32% of residues are conserved in all four compared sequences. 4% of the residues are unique in ML-I and conserved in the three other proteins as well. Among the 30 residues forming the PA cavity in ML-I 12% for the A-subunit and 27% of the B-subunit are conserved in all four lectins. It is interesting that conserved residues are not found in the PA-binding site, as shown in Fig. 3, and only non-conserved residues are located at the cavity surface, forming interactions with PA.

A further interesting feature of the amino acid substitutions is, that three residues of ricin are near to the surface entrance of the cavity. These residues are Phe240A, Phe140B, and Phe262B with the side chains arranged in a propeller type shape. This orientation describes the energetically favorable conformation designated as ''edge-to-face'' [29]. Consequently, the bulky aromatic rings restrict access to the cavity and it is unlikely that ligands can enter and bind in the cavity as found for ML-I where the corresponding residues are Val228A, Arg388B, and Pro510B located close to the entrance of the cavity.

The X-ray structures of native ML-I and in a complex with adenine have been published before [10] and the depurination activity of ML-I chain A towards adenine 4324 of the 28S rRNA has been described based on the X-ray structures. Also, the sugar-binding sites of the B chain have been characterized based on the X-ray structure of ML-I with bound galactose [30]. Here we present the three-dimensional structure of a co-crystallized complex of ML-I with PA that reveals a new binding site. It is located between chains A and B, and 25 Å far from the active site as well as 24 Å far from the galactose binding site I and II, respectively. We identified distinct H-bond interactions between PA and the protein, however the binding pocket is mainly hydrophobic, so it is possible that other small molecules with similar structures can also bind. PA binds

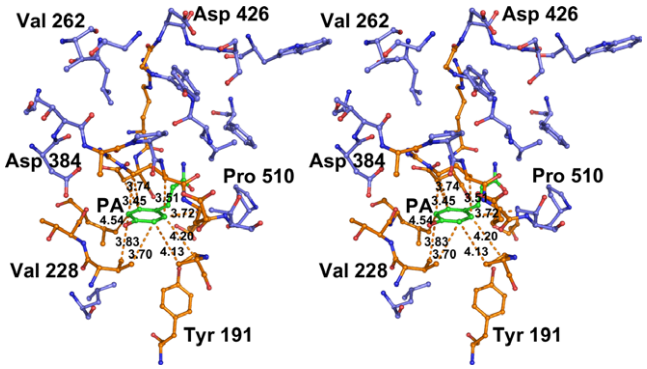

Fig. 3. Stereo view comparing the residues in the binding pocket. Residues that are either fully conserved in all four compared lectins or similar in hydrophobic properties are shown in medium blue. These residues are mostly located together, on the opposite side of the calculated cavity within the B-subunit away from the PA-binding site. Red colored residues are either different in all four lectins (Val228 is an exception because ebulin A here also has a Val) or unique in ML-I but the same in two or three other lectins. These residues are clustered around the entrance of the cavity. Not all residues contribute to the PA binding, which opens the possibility that other ligands may also bind in this pocket. (For interpretation of the references to colors in this figure legend, the reader is referred to the web version of this article.)

at the hydrophobic access of the cavity and the residues that participate in the binding are mostly unique to ML-I or at least less conserved in ML-I than in known lectins from non-parasitic organisms. The distribution of non-conserved and conserved residues seems to be more than just random.

It is evident that in the course of co-evolution mistletoe has acquired the ability to protect itself from hormone-mediated processes of the host. It is likely that PA contributes to the blossom development of the host during spring time. However, mistletoe blooms in late autumn. Also, being an evergreen plant the mistletoe is unimpaired by release of the host for the leaf shrivel. There are three possibilities for mistletoe to evade the host activity. Either, its tissues are insensitive to the host hormones, or small regulatory molecules are unable to pass through barriers between the parasite and the host, or the mistletoe has a mechanism to neutralize absorbed hormones. A combination of all three mechanisms is possible. ML-I may be an interceptor for host hormones. This implies that there should be some characteristic features in the hormone binding region of ML-I, compared to RIP-type II lectins from non-parasitic plants, e.g. ricin, abrin A or ebulin I.

In the course of evolution ML-I may have acquired additional functions, beside the defense function of a RIP-type II Protein. It is also possible that the interaction of ML-I with PA is biologically irrelevant and the PA-binding cavity is merely a space between two connected amino acid chains. However, ordered interactions between molecules that are highly active, with major physiological consequences, are unlikely to occur fortuitously between organisms connected as intimately as a parasite and its host. Therefore, the identified interaction between ML-I and PA is most probably biologically meaningful. ML-I's role could be to intercept or to carry the host hormone.

Acknowledgments

The work was supported by grants from the Deutsche Luft- und Raumfahrtagentur (DLR under Project No. 50WB0615), from the RiNA GmbH (Berlin) and DFG via Grant BUL 436/111/2007.

References

[1] W. Voelter, R. Wacker, S. Stoeva, R. Tsitsilonis, C. Betzel, Mistletoe lectins, structure and function, Front. Nat. Prod. Chem. 1 (2005) 149–162.

[2] Y. Endo, Y. Chan, A. Lin, K. Tsurugi, I.G. Wool, The cytotoxins alpha-sarcin and ricin retain their specificity when tested on a synthetic oligoribonucleotide (35-mer) that mimics a region of 28 S ribosomal ribonucleic acid, J. Biol. Chem. 263 (1988) 7917–7920.

[3] K. Nielsen, R.S. Boston, Ribosome-inactivating proteins: a plant perspective, Annu. Rev. Plant Physiol. Plant Mol. Biol. 52 (2001) 785–816.

[4] J. Eck, M. Langer, B. Möckel, A. Baur, M. Rothe, H. Zinke, H. Lentzen, Cloning of the mistletoe lectin gene and characterization of the recombinant A-chain, Eur. J. Biochem. 264 (1999) 775–784.

[5] J.T. Fisher, Water relations of mistletoes and their hosts, in: M. Calder, P. Bernhardt (Eds.), The Biology of Mistletoes, Acad. Press, Sydney, 1983, pp. 161–184.

[6] I. Ullmann, L.O. Lange, H. Ziegler, J. Ehleringer, E.D. Schulze, I.R. Cowan, Diurnal courses of leaf conductance and transpiration of mistletoes and their hosts in Central Australia, Oecologia 67 (1985) 577–587.

[7] M. Barberaki, S. Kintzios, Accumulation of selected macronutients in mistletoe tissue cultures: effect of medium composition and explant source, Sci. Hortic. 95 (2002) 133–150.

[8] C.F.v. Tubeuf, Monographie der Mistel, Druck und Verlag von R. Oldenburg, München und Berling, 1923.

[9] H. Rybicka, Phloretamide in fruitlets of apple tree (*Malus domestica*), Acta Physiol. Plant. 18 (1996) 359–363.

[10] R. Krauspenhaar, W. Rypniewski, N. Kalkura, K. Moore, L. DeLucas, S. Stoeva, A. Mikhailov, W. Voelter, C. Betzel, Crystallisation under microgravity of mistletoe lectin I from *Viscum album* with adenosine monophosphate and the crystal structure at 1.9 Å resolution, Acta Cryst. D 58 (2002) 1704–1707.

[11] R. Mikeska, R. Wacker, R. Arni, T.P. Singh, A. Mikhailov, A. Gabdoulkhakov, W. Voelter, C. Betzel, Mistletoe lectin I in complex with galactose and lactose reveals distinct sugar-binding properties, Acta Cryst. F 61 (2005) 17–25.

[12] S. Crider-Pirkle, P. Billingsley, C. Faust, D.M. Hardy, V. Lee, H. Weitlauf, Cubilin, a binding partner for galectin-3 in the murine utero-placental complex, J. Biol. Chem. 277 (2002) 15904–15912.

[13] Y. Li, U. Pfuller, E.L. Larsson, H. Jungvid, I.Y. Galaev, B. Mattiasson, Separation of mistletoe lectins based on the degree of glycosylation using boronate affinity chromatography, J. Chromatogr. 925 (2001) 115–121.

[14] Z. Otwinowski, W. Minor, Processing of X-ray diffraction data collected in oscillation mode, in: C.W. Carter Jr., R.M. Sweet (Eds.), Methods in Enzymology, Volume 276: Macromolecular Crystallography Part A, Academic Press, New York, 1997, pp. 307–326.

[15] B.W. Matthews, Solvent content of protein crystals, J. Mol. Biol. 33 (2) (1968) 491–497.

[16] G.N. Murshudov, A.A. Vagin, E.J. Dodson, Refinement of macromolecular structures by the maximum-likelihood method, Acta Cryst. D 53 (1997) 240–255.

[17] A.A. Vagin, R.A. Steiner, A.A. Lebedev, L. Potterton, S. McNicholas, F. Long, G.N. Murshudov, Refmac5 dictionary: organization of prior chemical knowledge and guidelines for its use, Acta Crystallogr. D Biol. Crystallogr. 60 (2004) 2184–2195.

[18] A.V. Lyashenko, N.E. Zhukhlistova, A.G. Gabdoulkhakov, Y.N. Zhukova, W. Voelter, V.N. Zaitsev, I. Bento, E.V. Stepanova, G.S. Kachalova, O.V. Koroleva, E.A. Cherkashyn, V.I. Tishkov, V.S. Lamzin, K. Schirwitz, E.Y. Morqunova, C. Betzel, P.F. Lindley, A.M. Mikhailov, Purification, crystallization and preliminary X-ray study of the fungal laccase from Cerrena maxima, Acta Cryst. F 62 (2006) 954–957.

[19] P. Emsley, K. Cowtan, Coot: model-building tools for molecular graphics, Acta Crystallogr. D Biol. Crystallogr. 60 (2004) 2126–2132.

[20] R.A. Laskowski, M.W. MacArthur, D.S. Moss, J.M. Thornton, Procheck: a program to check the stereochemical quality of protein structures, J. Appl. Cryst. 26 (1993) 283–291.

[21] SYBYL, Department of Chemistry, University of Cambridge, Lensfield Road, Cambridge CB2 1EW, 2005.

[22] R. Chenna, H. Sugawara, T. Koike, R. Lopez, T.J. Gibson, D.G. Higgins, J.D. Thompson, Multiple sequence alignment with the Clustal series of programs, Nucleic Acids Res. 31 (2003) 3497–3500.

[23] ACD/ChemSketch Freeware, Version 10.00, Advanced Chemistry Development Inc., Toronto, ON, Canada, 2006. Available from: <http://www.acdlabs.com>.

[24] CorelDraw/CorelPaint, Graphics Suite 12, Corel Corporation, Edisonstraße 6 85716, Unterschleißheim, Germany.

[25] J.E. Villafranca, J.D. Robertus, Ricin B chain is a product of gene duplication, J. Biol. Chem. 256 (1981) 554–556.

[26] J.M. Pascal, J.P. Day, A.F. Monzingo, S.R. Ernst, J.D. Robertus, R. Iglesias, Y. Pérez, J.M. Férreras, L. Citores, T. Gibés, 2.8-Å crystal structure of a non-toxic type-II ribosome-inactivating protein, ebulin I, Proteins Struct. Funct. Genet. 43 (3) (2001) 319–326.
[27] E. Rutenber, B.J. Katzin, S. Ernst, E.J. Collins, D. Mlsna, M.P. Ready, J.D. Robertus, Crystallographic Refinement of ricin to 2.5 Å, Proteins Struct. Funct. Genet. 10 (3) (1991) 240–250.
[28] T.H. Tahirov, T.H. Lu, Y.C. Liaw, Y.L. Chen, J.Y. Lin, Crystal structure of abrin-a at 2.14 Å, J. Mol. Biol. 250 (3) (1995) 354–367.
[29] S.K. Burley, G.A. Petsko, Aromatic–aromatic interaction: a mechanism of protein structure stabilization, Science 229 (4708) (1985) 23–28.
[30] H. Niwa, A.G. Tonevitsky, I.I. Agapov, S. Saward, U. Pfüller, R.A. Palmer, Crystal structure at 3 Å of mistletoe lectin I, a dimeric type-II ribosome-inactivating protein, complexed with galactose, Eur. J. Biochem. 270 (2003) 2739–2749.